ISBN: 978-3-95450-200-4 doi:10.18429/JACoW-ICAP2018-TUPAG07

EFFICIENT COMPUTATION OF LOSSY HIGHER ORDER MODES IN COMPLEX SRF CAVITIES USING REDUCED ORDER MODELS AND NONLINEAR EIGENVALUE PROBLEM ALGORITHMS*

H. W. Pommerenke†, J. D. Heller, U. van Rienen[1]
Institute of General Electrical Engineering, University of Rostock, Germany
[1]also at Department Life, Light & Matter, University of Rostock, Germany

Abstract

Superconducting radio frequency (SRF) cavities meet the demanding performance requirements of modern accelerators and high-brilliance light sources. For the operation and design of such resonators, a very precise knowledge of their electromagnetic resonances is required. The non-trivial cavity shape demands a numerical solution of Maxwell's equations to compute the resonant eigenfrequencies, eigenmodes, and their losses. For large and complex structures this is hardly possible on conventional hardware due to the high number of degrees of freedom required to obtain an accurate solution. In previous work it has been shown that the considered problems can be solved on workstation computers without extensive simplification of the structure itself by a combination of State-Space Concatenation (SSC) and Newton iteration to solve the arising nonlinear eigenvalue problem (NLEVP).

First, SSC is applied to the complex, closed and thus lossless RF structure. SSC employs a combination of model order reduction and domain decomposition, greatly reducing the computational effort by effectively limiting the considered frequency domain. Next, a perturbation approach based on SSC is used to describe the resonances of the same geometry subject to external losses. This results in a NLEVP which can be solved efficiently by Newton's method. In this paper, we expand the NLEVP solution algorithm by a contour integral technique, which increases the completeness of the solution set.

INTRODUCTION

Superconducting radio frequency (SRF) cavities are essential components of modern particle accelerators, as they provide the radio frequency (RF) electromagnetic fields used to accelerate charged particles to high energies. The design of RF cavities requires a precise knowledge of their resonant frequencies f, field distributions, and power losses P. This usually requires solving an eigenvalue problem, where the eigenvalues and eigenvectors correspond to the frequencies and field distributions, respectively. In this context, the eigenvectors are also denoted as eigenmodes of the cavity.

A dimensionless measure for power losses in general is the quality factor

$$Q = 2\pi f W/P, \tag{1}$$

which is the ratio between the energy loss per oscillation and the total energy W stored in the electromagnetic field. Generally, there are dielectric, magnetic, surface and external losses. The latter occur when energy is propagating out of the cavity through its openings, e.g. a coupler or the beam pipe. For an SRF cavity, the external losses are several orders of magnitude larger than other loss mechanisms, since the structure is both superconducting and evacuated [1]. Therefore, the external quality factor Q_{ext} is often equivalent to the total Q (and in the following denoted as such). External losses are of significant importance for eigenmodes, whose resonant frequencies are larger than that of the operating mode used for acceleration. They are denoted as higher order modes (HOM). These usually unwanted modes are excited by the current of the passing beam and may influence the beam in an unwanted manner, e.g. by deviation from its optimum trajectory or emittance growth [2, 3]. One usually designs cavities such that HOM energy is dissipated quickly and the mode is practically completely damped before the next particle bunch arrives. The structures must thus feature low Q factors regarding the HOMs. Besides available openings like the beam pipe or the power coupler, HOM couplers are utilized. Nevertheless, there exist additional HOMs whose interaction with the couplers is almost non-existent and which therefore have very high Q factors. Identification and computation of these trapped modes is particularly important in SRF cavity design [1, 4, 5].

Even for comparatively simple structures, an analytical solution of Maxwell's equations [6] is not available. Numerical methods such as the Finite Element Method (FEM) [7] or Finite Integration Technique (FIT) [8, 9] are therefore employed. If one solely considers closed lossless cavities, this leads to a linear eigenvalue problem (LEVP), whose solution can be acquired by a variety of methods. However, the precise computation of external losses is accomplished by applying suitable boundary conditions to the cavity's openings leading to a complex-valued, nonlinear eigenvalue problem (NLEVP), whose solution requires significantly more effort.

The above-mentioned numerical methods show disadvantageous scaling behavior regarding size and complexity of the structure. Especially large and complex structures, e.g. a sequence of cavities and couplers like in Fig. 1, require many degrees of freedom (DOF) for an accurate solution. In a direct approach, these problems can only be solved on powerful computational infrastructure which is costly and rarely available. Another possibility is to only con-

* This work has been supported by the German Federal Ministry of Education and Research (grant no. 05K13HR1).
† Currently also at CERN, Geneva, Switzerland.
Email: hermann.pommerenke@uni-rostock.de

ISBN: 978-3-95450-200-4 doi:10.18429/JACoW-ICAP2018-TUPAG07

sider a part of the structure by restricting the computational domain. While this approach is suitable if the fields are confined in one cavity, a significant portion of HOM energy is stored in electromagnetic fields that may fill the entire structure [1] (Fig. 1(b)). Such fields cannot be computed if the domain is limited to a single cavity.

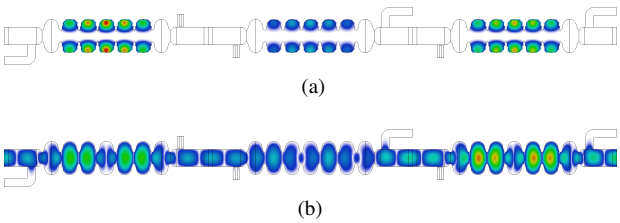

(a)

(b)

Figure 1: Electric field of two HOMs of the bERLinPro linac [10]. (a) Mode resonating at 3.68 GHz that is confined within the cavities. (b) Mode resonating at 1.86 GHz with a field distribution filling the entire structure. The plots are taken from [11].

In [11] it was shown by Heller that employing the State-Space Concatenation Scheme (SSC) [12, 13] together with suitable boundary conditions leads to a NLEVP which can be solved efficiently by Newton's method [14]. In this paper, we extend upon these results by combining them with a contour integral algorithm proposed by Beyn [15] to increase the completeness of the solution set. The proposed technique has been used to investigate current examples from accelerator physics.

STATE-SPACE CONCATENATION

SSC has been suggested by Flisgen [12, 13] and is a combination of domain decomposition and model order reduction (MOR) techniques to solve Maxwell's equations for large complex SRF structures. We will introduce it briefly here; for an exhaustive explanation we refer to [13, 16–18].

First, the investigated structure is decomposed into non-overlapping segments. The substructures are treated separately, with the cutting planes considered as waveguide ports. For each segment, a State-Space model (SSM) is assembled. An incomplete eigendecomposition is performed, computing a finite number[1] of 3D eigenmodes around the frequency interval of interest. Due to poor convergence of the incomplete decomposition, a very high number of modes would be necessary, since even the structure's behavior within a certain frequency range is influenced by modes outside said range. Instead, the orthogonal basis is expanded by so-called snapshots computed from the frequency response of the segment to certain excitations. This is done for a total of N_{3D} modes. This technique is denoted as Corrected Modal Expansion (CME) [17]. The 3D modes represent the internal states of the system comprised in the state vector $\boldsymbol{x}$. For each waveguide port, 2D port modes are computed, with N_{2D} denoting the total number of port modes of the segment.

[1] The amount of 3D eigenmodes is by orders of magnitude smaller than the DOFs.

Their amplitudes are comprised in the vector of modal currents $\boldsymbol{i}$ and modal voltages $\boldsymbol{v}$. The coupling between 3D eigenmodes and 2D port modes is obtained as the inner product of the respective fields. In frequency domain, the assembled first-order SSM[2] reads as

$$\begin{aligned} s\boldsymbol{x}(s) &= \boldsymbol{A}\boldsymbol{x}(s) + \boldsymbol{B}\boldsymbol{i}(s) \\ \boldsymbol{v}(s) &= \boldsymbol{C}\boldsymbol{x}(s), \end{aligned} \tag{2}$$

with $\boldsymbol{A} \in \mathbb{R}^{2N_{3D}\times 2N_{3D}}$, $\boldsymbol{B} \in \mathbb{R}^{2N_{3D}\times N_{2D}}$ and $\boldsymbol{C} = \boldsymbol{B}^{\mathrm{T}}$.

The individual SSMs of the segments are concatenated by assembling $\boldsymbol{A}$, $\boldsymbol{B}$, and $\boldsymbol{C}$ from (2) into block matrices. Redundant modal currents and voltages at connected ports are eliminated using Kirchhoff's laws, so that only those of external ports remain. The MOR by CME is again applied to the concatenated SSM, further reducing the DOFs. The resulting reduced SSM of the complex structure is again of the same form as (2). The external modal currents and voltages can be used to assign excitations or boundary conditions to the structure.

SSC is not the only Maxwell solution approach involving a domain decomposition and concatenation approach. Notable methods are the mode-matching techniques e.g. [4, 5, 19–22], the Coupled S-Parameter Calculation [18, 23–25], the Generalized Scattering Matrix approach [26–28] or the description of RF structures by means of circuit theory, e.g. [17, 29]. However, to the best of the authors' knowledge, only SSC allows simultaneous and direct access to time and frequency domain calculations, MOR and 3D field distributions [11–13].

EXTERNAL LOSSES IN SRF CAVITIES

For the computation of external losses of an SRF cavity, the openings are modeled as having infinitely long waveguides attached to them, i.e. being reflection-free. Therefore impedance matching is required: the termination impedance (i.e. the quotient of modal voltage and current) of each port mode must be the wave impedance of said mode [30].

Each eigenmode of the lossy structure is described as a weighted sum of the eigenmodes of the corresponding lossless structure. In this perturbation ansatz usually one of the lossless eigenmodes dominates. For the description of certain perturbations, very high frequencies are necessary; in that case a large number of lossless eigenmodes must be considered in the preceding MOR. The resulting NLEVP read as [11, 16, 30]

$$\boldsymbol{T}(\lambda)\boldsymbol{x} = \left(\boldsymbol{A} - \boldsymbol{B}\boldsymbol{G}(\lambda)\boldsymbol{B}^{\mathrm{T}} - \lambda\boldsymbol{I}\right)\boldsymbol{x} = \boldsymbol{0}, \tag{3}$$

where λ and $\boldsymbol{x}$ denote the eigenvalue and eigenvector, respectively. The individual frequencies and external Q factors are obtained by

$$f = \frac{\Im\{\lambda\}}{2\pi} \qquad Q = -\frac{\Im\{\lambda\}}{2\Re\{\lambda\}}, \tag{4}$$

[2] The SSM may also be assembled as a symmetric second order system with half the degrees of freedom. Both can also be represented in time domain.

ISBN: 978-3-95450-200-4 doi:10.18429/JACoW-ICAP2018-TUPAG07

while the field distributions can be reconstructed from the respective eigenvectors.

The diagonal matrix $\boldsymbol{G}(\lambda)$ contains the reciprocal wave impedances (i.e. wave admittances) of the port modes which depend nonlinearly on the eigenvalues and are given for transversal electric (TE) and magnetic (TM) port modes by [31]

$$\begin{aligned} Z_{\text{wave}}^{\text{TE}}(\lambda) &= Z_0 \frac{\lambda}{\sqrt{\lambda^2 + \omega_{\text{co}}^2}} \\ Z_{\text{wave}}^{\text{TM}}(\lambda) &= Z_0 \frac{\sqrt{\lambda^2 + \omega_{\text{co}}^2}}{\lambda}, \end{aligned} \tag{5}$$

where $Z_0 \approx 377\,\Omega$ is the impedance of free space and ω_{co} denotes the cutoff frequency of the respective port mode. For transversal electromagnetic (TEM) waves this is the impedance of the connected transmission line, usually $Z_{\text{wave}}^{\text{TEM}} = 50\,\Omega$.

The introduction of the wave impedances (5) causes the operator $\boldsymbol{T}(\lambda)$ to be both nonlinear and meromorphic: isolated poles occur at $\lambda = 0$ and at the cutoff frequencies $\omega_{\text{co}}^{\text{TM}}$ of the TM port modes.

SOLVING THE NLEVP

The solution of NLEVPs $\boldsymbol{T}(\lambda)\boldsymbol{x} = \boldsymbol{0}$ such as (3) is significantly more demanding than that of well-known LEVPs, for which a wide range of solution methods exist [32–34]. The NLEVP is subject of active ongoing research. An overview over NLEVP solution approaches is given by [33, 35–39], notably the Newton iteration [14], contour integral methods [15, 40], or methods based on generalized QR decompositions [41] or Rayleigh functionals [42, 43].

In this work, we utilized Newton's method as well as a contour integral algorithm suggested by Beyn [15]. Both are introduced in the following.

Newton's Method

The well-known Newton's method [14] is used to successively approximate zeros of functions or operators. Solving the NLEVP (3) can be interpreted as finding zeros of $\boldsymbol{T}(\lambda)\boldsymbol{x}$ in an $(N+1)$-dimensional search space, where all components of the eigenvector $\boldsymbol{x} \in \mathbb{C}^N$ and the eigenvalue λ itself must be determined. Hence, a suitable formulation of the Newton iteration can be found [33, 36, 37].

Without loss of generality, the eigenvector is normalized according to $\boldsymbol{v}^{\text{H}}\boldsymbol{x} = 1$ and (3) is reformulated to

$$\boldsymbol{P}\begin{pmatrix}\boldsymbol{x}\\ \lambda\end{pmatrix} = \begin{pmatrix}\boldsymbol{T}(\lambda)\boldsymbol{x}\\ \boldsymbol{v}^{\text{H}}\boldsymbol{x} - 1\end{pmatrix} = \boldsymbol{0}. \tag{6}$$

Applying the iteration rule yields

$$\begin{pmatrix}\boldsymbol{x}_{\nu+1}\\ \lambda_{\nu+1}\end{pmatrix} = \begin{pmatrix}\boldsymbol{x}_{\nu}\\ \lambda_{\nu}\end{pmatrix} - \left(\boldsymbol{P}'\begin{pmatrix}\boldsymbol{x}_{\nu}\\ \lambda_{\nu}\end{pmatrix}\right)^{-1} \boldsymbol{P}\begin{pmatrix}\boldsymbol{x}_{\nu}\\ \lambda_{\nu}\end{pmatrix}, \tag{7}$$

where ν denotes the iteration index and $\boldsymbol{P}'$ is called Fréchet derivative [44] of $\boldsymbol{P}$. The initial pair $(\lambda_0, \boldsymbol{x}_0)$ must be known a priori. The initial pairs are usually obtained by solving a linearized system or (additionally) sampling the domain of interest using a grid or Monte Carlo methods.

As (7) is difficult to implement, one introduces the search direction $\boldsymbol{u}$ as an auxiliary quantity from which the approximated eigensolution is computed:

$$\begin{aligned} \boldsymbol{u}_{\nu+1} &= \boldsymbol{T}^{-1}(\lambda_\nu)\frac{\partial \boldsymbol{T}}{\partial \lambda}(\lambda_\nu)\boldsymbol{x}_\nu \\ \boldsymbol{x}_{\nu+1} &= c_{\nu+1}\boldsymbol{u}_{\nu+1} \\ \lambda_{\nu+1} &= \lambda_\nu - \frac{\boldsymbol{v}^{\text{H}}\boldsymbol{x}_\nu}{\boldsymbol{v}^{\text{H}}\boldsymbol{u}_{\nu+1}}, \end{aligned} \tag{8}$$

where c_ν is a normalization factor that influences the convergence speed[3]. In general, the iteration (8) stops when an error measure falls below a certain limit[4].

When employing Newton's method, convergence against previously computed eigenpairs must be avoided, which is called deflation. Most techniques of the LEVP solvers cannot be used [33], since the eigenvectors of the NLEVP are generally linearly dependent. A possibility is to choose $\boldsymbol{v}$ in each new solution attempt orthogonal to all previously computed eigenvectors. More sophisticated deflation techniques can be developed based on minimal invariant pairs, requiring an alternative formulation of the algorithm [39].

Beyn's Algorithm

The integral algorithm introduced by Beyn [15] allows for a complete solution of a NLEVP within a finite enclosed sub domain of the complex plane. We explain it briefly and refer to [15, 45, 46] for a detailed derivation.

The algorithm is based on Keldyš's theorem [45] stating that the inverse of $\boldsymbol{T}(z)$ may be expanded into a Laurent series, whose principal part can be expressed in terms of the right and left eigenvectors $\boldsymbol{x}, \boldsymbol{y}$ belonging to λ:

$$\boldsymbol{T}^{-1}(z) = \sum_{j=1}^{k} \frac{1}{z - \lambda_j}\boldsymbol{x}_j\boldsymbol{y}_j + (\text{holomorphic part}). \tag{9}$$

Choosing a rectangular matrix $\boldsymbol{\Psi}$ at random, the integrals

$$\boldsymbol{L}_p = \frac{1}{2\pi \text{j}} \oint_\Gamma z^p \boldsymbol{T}^{-1}(z)\boldsymbol{\Psi}\,\text{d}z \quad , \quad p = 0, 1 \tag{10}$$

are computed using numerical integration along a closed contour Γ. The computational cost is dominated by solving the linear system $\boldsymbol{T}^{-1}(z)\boldsymbol{\Psi}$ at every quadrature sampling point. The convergence behavior depends on the condition of the operator $\boldsymbol{T}(z)$, the number of sampling points, and chosen quadrature rule [15, 47, 48].

From (9) it follows by Cauchy's integral formula [34] that $\boldsymbol{L}_0 = \boldsymbol{X}\boldsymbol{Y}\boldsymbol{\Psi}$ and $\boldsymbol{L}_1 = \boldsymbol{X}\boldsymbol{\Lambda}\boldsymbol{Y}\boldsymbol{\Psi}$. The matrices $\boldsymbol{X}$, $\boldsymbol{Y}$ and

[3] In practice one choses e.g. $c_\nu = 1/||\boldsymbol{u}_\nu||$; however it has been observed that $|c_\nu| \ll 1$ leads to instability of the algorithm in rare cases. In [33] the condition $|c_\nu| < 1$ is mentioned to guarantee convergence.

[4] To account for potentially occurring non-convergence, the algorithm should additionally be stopped when a maximum number of iterations is reached.

ISBN: 978-3-95450-200-4 doi:10.18429/JACoW-ICAP2018-TUPAG07

Λ contain the left and right eigenvectors and eigenvalues, respectively, that are enclosed by Γ, but are independent of the specific contour shape. They are extracted using singular value decomposition.

In this work, we combine Beyn's algorithm with a subsequent Newton iteration to improve convergence as suggested in [36, 38], since the algorithm on its own shows disadvantageous convergence behavior when employed to the SRF cavity NLEVP. The solutions found by Beyn's algorithm are used as starting pairs for Newton's method. This has initially been tested in [48] and is demonstrated below.

The alternative Contour Integral Slicing Method proposed by [40] should also be acknowledged. It is available within the SLEPc library [49] combined with a Newton iteration in a similar fashion.

APPLICATION EXAMPLES

In the current setup implemented in [11], the SRF structure is discretized by FIT in CST Microwave Studio (CST MWS) [50]. The assembled matrices are transferred to and further processed in MATLAB [51] using a collection of scripts written in Python [52] and Visual Basic for Applications. The arising linear systems and decompositions are computed using linear algebra software packages like LAPACK [53] and ARPACK [54], which are made available by MATLAB and the Python packages NumPy [55] and SciPy [56]. The field plots are generated using Paraview [57].

All mentioned computations have been performed on an Intel Xeon E5-2687W CPU with 3.4 GHz clock rate, 256 GB RAM and Windows Server 2012.

Academic Example

The hypothetical minimalistic resonator depicted in Fig. 2 serves as a proof of principle. The cavity has two waveguide ports symbolizing a beam pipe and a HOM coupler. The structure is discretized in CST MWS using FIT with 233,000 mesh cells and Perfect Boundary Approximation [58]; after the MOR the arising NLEVP is of order $N = 178$.

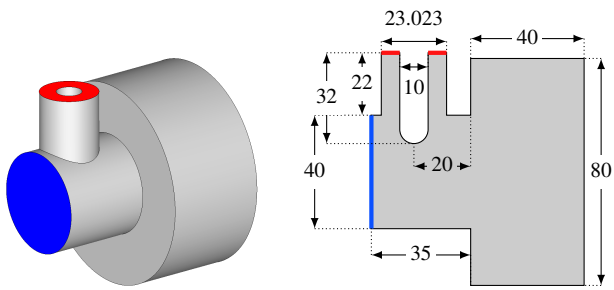

Figure 2: CAD model and sketch of the minimalistic resonator used as an academic example [11, 48]. Beam pipe and HOM coupler are highlighted in blue and red respectively. Geometric dimensions in mm.

Figure 3 shows the convergence behavior of Beyn's algorithm applied to this example with different numbers of quadrature points N_{Quad}. The relative residual

$$r_n = \frac{||\boldsymbol{T}(\lambda_n)\boldsymbol{x}_n||}{||\boldsymbol{x}_n||} \tag{11}$$

is used as an error measure. Even for very large N_{Quad}, the residual cannot be reduced below a certain limit. However, the convergence can drastically be improved by employing Newton's method. For comparison, reference solutions are computed from the scattering parameters of the structure using pole fitting [11, 59, 60].

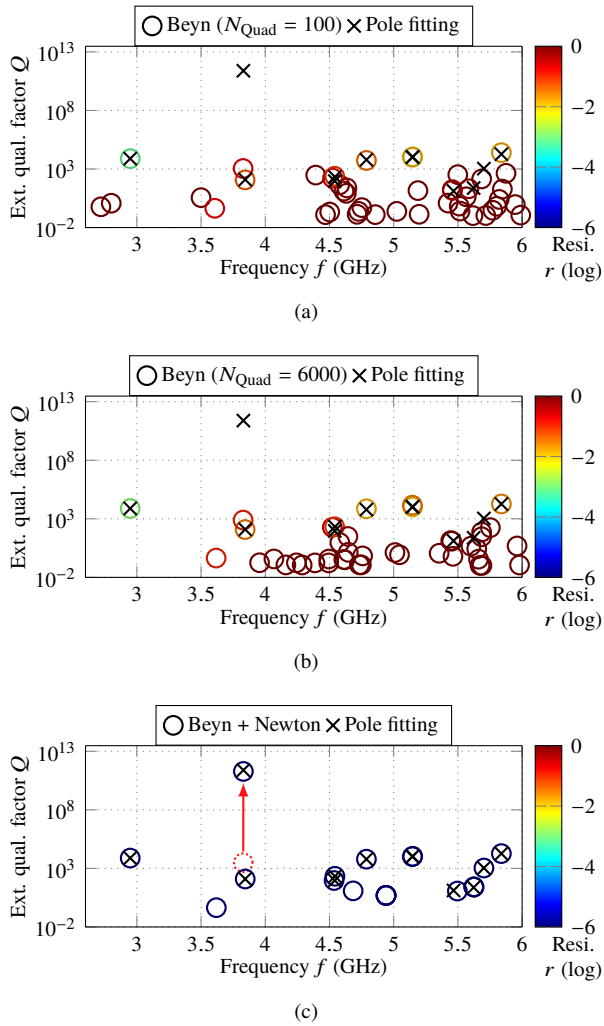

Figure 3: Eigensolutions of the minimalistic resonator with corresponding residuals r computed using Beyn's algorithm with different numbers of quadrature points: (a) $N_{\text{Quad}} = 100$, (b) $N_{\text{Quad}} = 6000$. The residual does not decrease for larger numbers of points, but can be further reduced by consecutive Newton iteration (c).

The time consumption of different setups is depicted in Fig. 4. The Newton iteration on its own computes solutions individually and fast, but without guaranteeing completeness. Employing Beyn's algorithm with comparably low numbers of quadrature points and using its solution as initial values for the Newton iteration yields the optimum solution strategy for this structure.

ISBN: 978-3-95450-200-4 doi:10.18429/JACoW-ICAP2018-TUPAG07

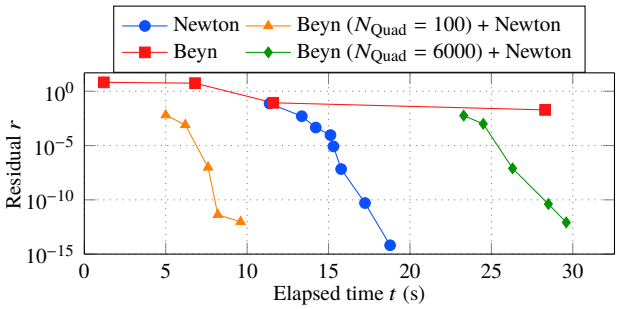

Figure 4: Time consumption of the different algorithms when solving the NLEVP of the minimalistic resonator.

FLASH Third Harmonic Cavity

The SRF structure depicted in Fig. 5 is part of the Third Harmonic Module [61, 62] of the Free Electron Laser in Hamburg (FLASH). It consists of a nine-cell 3.9 GHz cavity, an input coupler and two HOM couplers. For the MOR by SSC, it is decomposed into three segments. Due to the three couplers in addition to the beam pipe, five external waveguide ports are defined, and the NLEVP is of order $N = 780$.

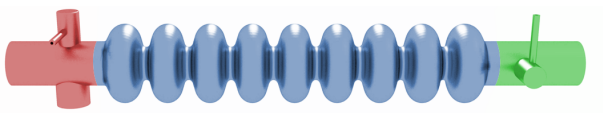

Figure 5: CAD model of the FLASH cavity. The colors indicate the chosen domain decomposition for SSC.

Figure 6(a) shows the results obtained by Beyn's algorithm with $N_{\mathrm{Quad}} = 2000$ quadrature points and the corresponding residuals. While for most higher-Q modes an acceptable residual is achieved, the lower-Q modes do not converge even for by orders of magnitude larger N_{Quad} ($10^{-1} \leq r \leq 10^{-4}$). We can again improve the eigensolutions by individual Newton iteration. To achieve a residual below 10^{-5} down to 10^{-10}, 4 min are required by Beyn's algorithm, whereas the Newton iteration consumes an additional 6 min. The corresponding solutions are shown in Fig. 6(b). Especially in the more relevant cases of larger Q factors, i.e. potentially dangerous parasitic eigenmodes, a very good agreement is observed with the pole fitting solutions [11, 59, 60].

Next we compare the eigensolutions of the FLASH cavity found by Newton's method alone and when combined with Beyn's algorithm. Figure 7 depicts the computed frequencies and external Q factors and the electric field of a few selected modes is shown in Fig. 8. Newton's method solves the NLEVP with residuals $10^{-5} \leq r \leq 10^{-10}$ in about 7 min. The combination of both algorithms finds a few additional solutions mainly in the low-Q range, but is slightly slower (10 min). The difference in computational speed by a few minutes when solving the NLEVP is insignificant compared to the time consumption of the preceding MOR: the generation of the reduced SSM of the concatenated structure[5] takes roughly 7 h. However, the MOR by SSC approach is much faster than alternative methods.

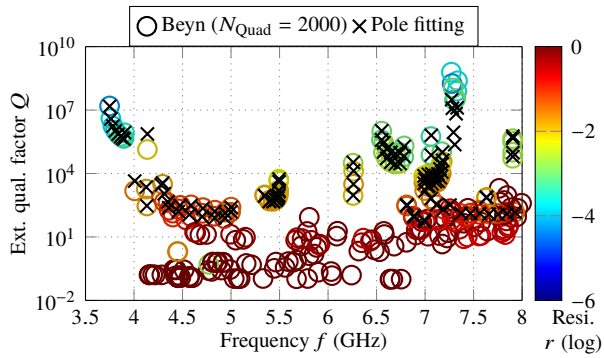

(a)

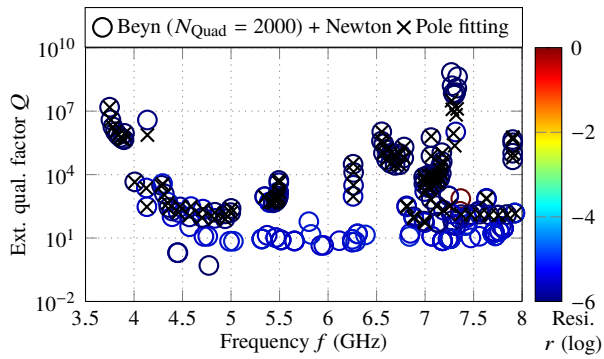

(b)

Figure 6: Computed frequencies and Q factors of the FLASH cavity with corresponding residuals r. (a) Solutions computed by Beyn's algorithm with $N_{\mathrm{Quad}} = 2000$ quadrature points. Even for much larger N_{Quad}, the residuals do not improve significantly. (b) The convergence can be improved for individual eigenmodes by employing Newton iteration.

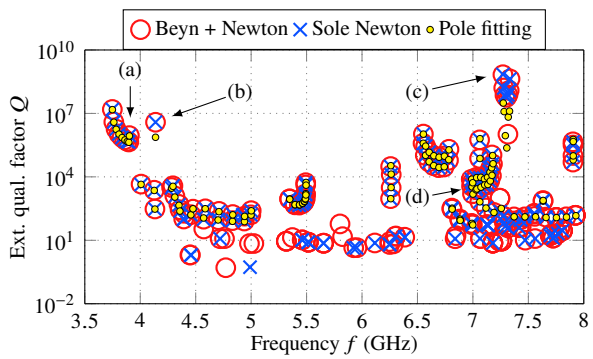

Figure 7: Eigensolutions of the FLASH cavity computed from the NLEVP by sole Newton iteration and by Beyn's algorithm with consecutive Newton iteration, with pole fitting solutions as reference. The markings (a)-(d) refer to the field distributions depicted in Fig. 8.

CONCLUSION

The method developed in [11–13] allows the computation of resonant frequencies, external losses and field distribu-

[5] The initial FIT mesh has roughly $3 \cdot 10^6$ DOF. 200 to 300 3D eigenmodes are computed in each segment. For the external waveguide ports 25 port modes are considered in total.

ISBN: 978-3-95450-200-4 doi:10.18429/JACoW-ICAP2018-TUPAG07

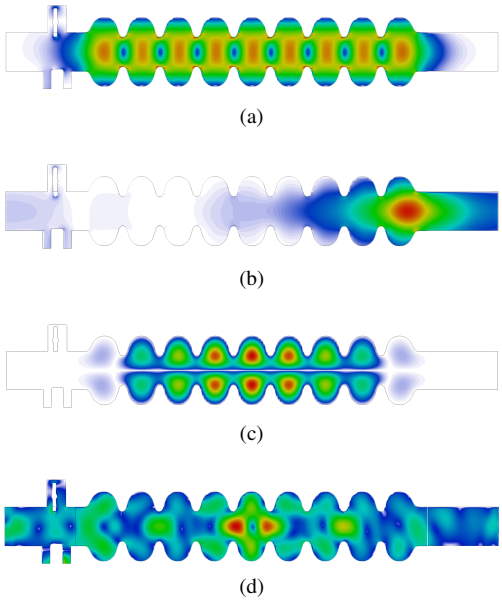

Figure 8: Electric fields of selected eigenmodes of the FLASH cavity: (a) Accelerating π-mode at 3.90 GHz. (b) Potentially dangerous trapped mode at 4.14 GHz with high Q and non-zero R/Q. (c) Trapped mode at 7.27 GHz and the highest Q within the analyzed spectrum. (d) Mode at 7.10 GHz with strong coupling to the cavity ports.

tion of complex SRF structures without extensive geometric simplification on workstation computers. The MOR and domain decomposition by SSC significantly reduce the computational effort. Using a perturbation approach and nonlinear boundary conditions, a NLEVP describing the external losses is obtained. The Newton iteration [14] can solve the arising NLEVP efficiently. This paper extends the approach by solving the NLEVP using Beyn's contour integral algorithm [15]. The convergence of this algorithm is observed to be limited for the type for NLEVP arising from SRF cavities. However, using it to compute initial eigenpairs for a consecutive Newton iteration shows promising results. More eigenmodes can be found in a comparable amount of time than by solely employing Newton's method. The approach has been demonstrated on an academic and a real-life SRF resonator.

REFERENCES

[1] H. Padamsee, J. Knobloch, and T. Hays, *RF Superconductivity: Science, Technology and Applications*. Wiley-WCH, 2008, ISBN: 9783527408429. DOI: 10 . 1002 / 9783527627172.

[2] S. U. de Silva and J. R. Delayen, "Wakefield analysis of superconducting rf-dipole cavities," in *Proceedings of the 28th Linear Accelerator Conference (LINAC'16), East Lansing, MI, USA*, 2017, pp. 206–208. DOI: 10.18429/JACoW-LINAC2016-MOPLR031.

[3] T. Weiland and R. Wanzenberg, "Wake fields and impedances," in *Frontiers of Particle Beams: Intensity Limitations*, Springer, 1992, pp. 39–79. DOI: 10.1007/3-540-55250-2_26.

[4] U. van Rienen, "Higher order mode analysis of tapered disc-loaded waveguides using the mode matching technique," *Particle Accelerators*, vol. 41, pp. 173–201, 1993.

[5] T. Weiland, U. van Rienen, P. Hülsmann, W. F. O. Müller, and H. Klein, "Investigations of trapped higher order modes using a 36-cell test structure," *Physical Review Special Topics-Accelerators and Beams*, vol. 2, no. 4, p. 042 001, 1999. DOI: 10.1103/PhysRevSTAB.2.042001.

[6] J. C. Maxwell, *A Treatise on Electricity and Magnetism*. Clarendon Press, 1873, ISBN: 9780511709333. DOI: 10 . 1017/cbo9780511709333.

[7] A. Bondeson, T. Rylander, and P. Ingelström, *Computational Electromagnetics*, ser. Texts in Applied Mathematics. Springer New York, 2005, ISBN: 9780387261584.

[8] T. Weiland, "A discretization model for the solution of Maxwell's equations for six-component fields," *AE Ü*, vol. 31, no. 3, pp. 116–120, 1977.

[9] U. van Rienen, *Numerical Methods in Computational Electrodynamics: Linear Systems in Practical Applications*, ser. Lecture Notes in Computational Science and Engineering. Springer Berlin Heidelberg, 2012, ISBN: 9783642568022.

[10] T. Galek, J. Heller, T. Flisgen, and U. van Rienen, *Report on ssc calculations for bERLinPro module containing three srf cavities*, Internal Document, 2016.

[11] J. D. Heller, "Numerical simulation of electromagnetic felds in complex multi-cavity superconducting radio frequency resonators," PhD thesis, Universität Rostock, 2018.

[12] T. Flisgen, H.-W. Glock, and U. van Rienen, "Compact time-domain models of complex rf structures based on the real eigenmodes of segments," *IEEE Transactions on Microwave Theory and Techniques*, vol. 61, no. 6, pp. 2282–2294, 2013. DOI: 10.1109/TMTT.2013.2260765.

[13] T. Flisgen, "Compact state-space models for complex superconducting radio-frequency structures based on model order reduction and concatenation methods," available as CERN-ACC-2015-0145, PhD thesis, University of Rostock, 2015.

[14] P. M. Anselone and L. B. Rall, "The solution of characteristic value-vector problems by Newton's method," *Numerische Mathematik*, vol. 11, no. 1, pp. 38–45, 1968. DOI: 10.1007/BF02165469.

[15] W.-J. Beyn, "An integral method for solving nonlinear eigenvalue problems," *Linear Algebra and Its Applications*, vol. 436, no. 10, pp. 3839–3863, 2012. DOI: 10.1016/j.laa.2011.03.030.

[16] T. Flisgen, A. Vélez, J. D. Heller, S. Zadeh, and U. van Rienen, "Computation of eigenmodes for the bessy vsr cavity chain by means of concatenation strategies," in *Proceedings of the 13th International Computational Accelerator Physics Conference (ICAP'18), Key West, FL, USA*, To appear, 2018.

[17] T. Wittig, *Zur Reduzierung der Modellordnung in elektromagnetischen Feldsimulationen*. Cuvillier Verlag, 2004, ISBN: 9783865372086.

[18] H.-W. Glock, K. Rothemund, and U. van Rienen, "CSC-A procedure for coupled S-parameter calculations," *IEEE Transactions on Magnetics*, vol. 38, no. 2, pp. 1173–1176, 2002. DOI: 10.1109/20.996300.

[19] E. Kühn, "A mode-matching method for solving field problems in waveguide and resonator circuits," *Archiv fuer Elektronik und Übertragungstechnik*, vol. 27, pp. 511–518, 1973.

[20] R. Mittra, Y. Hou, and V. Jamnejad, "Analysis of open dielectric waveguides using mode-matching technique and vari-

ISBN: 978-3-95450-200-4 doi:10.18429/JACoW-ICAP2018-TUPAG07

ational methods," *IEEE Transactions on Microwave Theory and Techniques*, vol. 28, no. 1, pp. 36–43, 1980. DOI: 10.1109/TMTT.1980.1130003.

[21] W. Wessel, T. Sieverding, and F. Arndt, "Mode-matching analysis of general waveguide multiport junctions," in *Microwave Symposium Digest, 1999 IEEE MTT-S International*, IEEE, vol. 3, 1999, pp. 1273–1276. DOI: 10.1109/MWSYM.1999.779619.

[22] S. J. Cooke, "Reduced-order simulation of large accelerator structures," *Physics of Plasmas*, vol. 15, no. 5, p. 056 706, 2008. DOI: 10.1063/1.2870086.

[23] K. Rothemund, D. Hecht, U. van Rienen, *et al.*, "Calculation of rf properties of the third harmonic cavity," in *Proceedings of the 22nd Linear Accelerator Conference (LINAC'04), Lübeck, Germany*, vol. 14243, 2004, p. 4.

[24] U. van Rienen, H.-W. Glock, D. Hecht, and K. Rothemund, "Computation of higher order modes in TESLA structures," *International Journal of Applied Electromagnetics and Mechanics*, vol. 14, no. 1-4, pp. 237–242, 2001.

[25] K. Rothemund, H.-W. Glock, and U. van Rienen, "Eigenmode calculation of complex rf-structures using s-parameters," *IEEE Transactions on Magnetics*, vol. 36, no. 4, pp. 1501–1503, 2000. DOI: 10.1109/20.877722.

[26] I. R. R. Shinton and R. M. Jones, "Large scale linac simulations using a globalised scattering matrix approach," in *Proceedings of the 11th European Particle Accelerator Conference (EPAC'08), Genoa, Italy*, 2008.

[27] I. R. R. Shinton, R. M. Jones, Z. Li, and P. Zhang, "Simulations of higher order modes in the ACC39 module of FLASH," in *3rd International Particle Accelerator Conference (IPAC'12), New Orleans, LA, USA*, 2012.

[28] R. M. Jones, L. Shi, and N. Baboi, "Simulation of electromagnetic scattering through the E-XFEL third harmonic cavity module," in *Proceedings of the 7th International Particle Accelerator Conference (IPAC'16), Busan, Korea*, 2016. DOI: 10.18429/JACoW-IPAC2016-WEPOY007.

[29] M. Liepe, "Superconducting multicell cavities for linear colliders," PhD thesis, Universität Hamburg, 2001.

[30] T. Flisgen, J. Heller, and U. van Rienen, "Time-domain absorbing boundary terminations for waveguide ports based on state-space models," *IEEE Transactions on Magnetics*, vol. 50, no. 2, pp. 145–148, 2014. DOI: 10.1109/TMAG.2013.2283065.

[31] T.-H. Loh and C. Mias, "Implementation of an exact modal absorbing boundary termination condition for the application of the finite-element time-domain technique to discontinuity problems in closed homogeneous waveguides," *IEEE Transactions on Microwave Theory and Techniques*, vol. 52, no. 3, pp. 882–888, 2004. DOI: 10.1109/TMTT.2004.823559.

[32] S. Börm and C. Mehl, *Numerical Methods for Eigenvalue Problems*, ser. De Gruyter Graduate Lectures. Walter de Gruyter, 2012, ISBN: 9783110250336. DOI: 10.1515/9783110250374.

[33] A. Ruhe, "Algorithms for the nonlinear eigenvalue problem," *SIAM Journal on Numerical Analysis*, vol. 10, no. 4, pp. 674–689, 1973. DOI: 10.1137/0710059.

[34] I. N. Bronshtein, K. A. Semendyayev, G. Musiol, and H. Mühlig, *Handbook of Mathematics*. Springer Berlin Heidelberg, 2015, ISBN: 9783662462218.

[35] Z. Bai, J. Demmel, J. Dongarra, A. Ruhe, and H. van der Vorst, *Templates for the Solution of Algebraic Eigenvalue Problems: a Practical Guide*. SIAM, 2000, ISBN: 9780898714715. DOI: 10.1137/1.9780898719581.

[36] H. Voss, "Nonlinear eigenvalue problems," in *Handbook of Linear Algebra*, vol. 164, Chapman and Hall/CRC Boca Raton, FL, 2013.

[37] V. Mehrmann and H. Voss, "Nonlinear eigenvalue problems: A challenge for modern eigenvalue methods," *GAMM-Mitteilungen*, vol. 27, no. 2, pp. 121–152, 2004. DOI: 10.1002/gamm.201490007.

[38] S. Güttel and F. Tisseur, "The nonlinear eigenvalue problem," *Acta Numerica*, vol. 26, pp. 1–94, 2017. DOI: 10.1017/S0962492917000034.

[39] C. Effenberger, "Robust solution methods for nonlinear eigenvalue problems," PhD thesis, École polytechnique fédérale de Lausanne, 2013.

[40] T. Sakurai and H. Sugiura, "A projection method for generalized eigenvalue problems using numerical integration," *Journal of Computational and Applied Mathematics*, vol. 159, no. 1, pp. 119–128, 2003. DOI: 10.1016/S0377-0427(03)00565-X.

[41] V. N. Kublanovskaja, "On an application of Newton's method to the determination of eigenvalues of λ-matrices," *Doklady Akademii Nauk SSSR*, vol. 188, pp. 1004–1005, 1969.

[42] R. J. Duffin, "A minimax theory for overdamped networks," *Journal of Rational Mechanics and Analysis*, vol. 4, pp. 221–233, 1955. DOI: 10.1512/iumj.1955.4.54007.

[43] K. P. Hadeler, "Mehrparametrige und nichtlineare Eigenwertaufgaben," *Archive for Rational Mechanics and Analysis*, vol. 27, no. 4, pp. 306–328, 1967. DOI: 10.1007/bf00281717.

[44] L. B. Rall, *Computational Solution of Nonlinear Operator Equations*. Wiley New York, 1969, ISBN: 9783110920291. DOI: 10.1515/9783110920291.

[45] M. V. Keldyš, "On the characteristic values and characteristic functions of certain classes of non-selfadjoint equations," *Doklady Akademii Nauk SSSR*, vol. 77, pp. 11–14, 1951.

[46] R. Mennicken and M. Möller, *Non-Self-Adjoint Boundary Eigenvalue Problems*, 1st ed., ser. North Holland Mathematics Studies. North Holland, 2003, vol. 192, ISBN: 9780444514479.

[47] L. N. Trefethen and J. A. C. Weideman, "The exponentially convergent trapezoidal rule," *SIAM Review*, vol. 56, no. 3, pp. 385–458, 2014. DOI: 10.1137/130932132.

[48] H. W. Pommerenke, "Untersuchung von konturintegralmethoden zur lokal vollständigen lösung nichtlinearer eigenwertprobleme, die auf den maxwell-gleichungen basieren," Master's thesis, Universität Rostock, 2017.

[49] V. Hernandez, J. E. Roman, and V. Vidal, "SLEPc: A scalable and flexible toolkit for the solution of eigenvalue problems," *ACM Trans. Math. Software*, vol. 31, no. 3, pp. 351–362, 2005. DOI: 10.1145/1089014.1089019.

[50] Computer Simulation Technology AG, *CST Studio Suite 2017*.

[51] T. M. Inc., *Matlab version r2015b*.

[52] G. van Rossum and F. L. Drake Jr., *Python Reference Manual*. Centrum voor Wiskunde en Informatica Amsterdam, 1995.

[53] E. Anderson *et al.*, *LAPACK Users' Guide*, 3rd ed. Society for Industrial and Applied Mathematics, 1999, ISBN: 0898714478. DOI: 10.1137/1.9780898719604.

[54] R. B. Lehoucq, D. C. Sorensen, and C. Yang, *ARPACK users' guide: Solution of large scale eigenvalue problems with implicitly restarted arnoldi methods*, Computer Based Learning Unit, University of Leeds, 1997. DOI: 10.1137/1.

ISBN: 978-3-95450-200-4 doi:10.18429/JACoW-ICAP2018-TUPAG07

9780898719628.

[55] S. van der Walt, S. C. Colbert, and G. Varoquaux, "The NumPy array: A structure for efficient numerical computation," *Computing in Science & Engineering*, vol. 13, no. 2, pp. 22–30, 2011. DOI: 10.1109/MCSE.2011.37.

[56] E. Jones, T. Oliphant, P. Peterson, *et al.*, *SciPy: Open source scientific tools for Python*, 2001. http://www.scipy.org

[57] A. Henderson, J. Ahrens, C. Law, *et al.*, *The ParaView Guide*. Kitware Clifton Park, NY, 2004, ISBN: 9781930934306.

[58] B. Krietenstein, P. Thoma, R. Schuhmann, and T. Weiland, "The perfect boundary approximation technique facing the big challenge of high precision computation," in *Proceedings of the 19th Linear Accelerator Conference (LINAC'98), Chicago, IL, USA*, 1998.

[59] T. Galek, T. Flisgen, U. van Rienen, B. Riemann, and A. Neumann, "Traveling poles elimination scheme and calculations of external quality factors of HOMs in SC cavities," in *Proceedings of the 11th International Computational Accelerator Physics Conference (ICAP'12), Rostock-Warnemünde, Germany*, 2012, pp. 152–154.

[60] B. Gustavsen, "Improving the pole relocating properties of vector fitting," *IEEE Transactions on Power Delivery*, vol. 21, no. 3, pp. 1587–1592, 2006. DOI: 10.1109/TPWRD.2005.860281.

[61] J. Sekutowicz, R. Wanzenberg, W. F. O. Müller, and T. Weiland, "A design of a 3rd harmonic cavity for the TTF 2 photoinjector," *DESY-TESLA-FEL*, vol. 5, p. 2002, 2002.

[62] N. Solyak *et al.*, "Development of the third harmonic sc cavity at fermilab," in *Proceedings of the Particle Accelerator Conference, Portland, OR, USA*, IEEE, vol. 2, 2003, pp. 1213–1215. DOI: 10.1109/PAC.2003.1289656.